ACS Chemical Neuroscience

Research Article

pubs.acs.org/chemneuro

Sex- and SERT-Mediated Differences in Stimulated Serotonin Revealed by Fast Microdialysis

Hongyan Yang,[†] Maureen M. Sampson,[†,‡,§] Damla Senturk,[∥] and Anne M. Andrews*[,†,‡,§]

[†]Department of Psychiatry & Biobehavioral Sciences, Hatos Center for Neuropharmacology, Semel Institute for Neuroscience & Human Behavior, David Geffen School of Medicine, [‡]Molecular Toxicology Interdepartmental Program, [§]Department of Chemistry & Biochemistry, and [∥]Department of Biostatistics, Fielding School of Public Health, University of California, Los Angeles, Los Angeles, California 90095, United States

Supporting Information

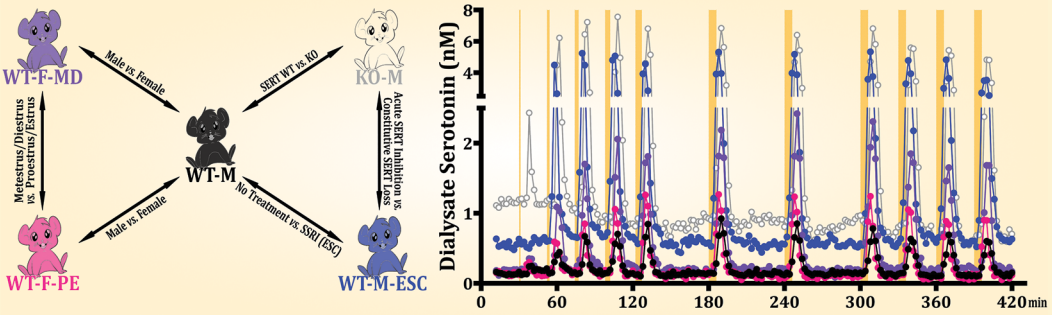

ABSTRACT: *In vivo* microdialysis is widely used to investigate how neurotransmitter levels in the brain respond to biologically relevant challenges. Here, we combined recent improvements in the temporal resolution of online sampling and analysis for serotonin with a brief high-K^+ stimulus paradigm to study the dynamics of evoked release. We observed stimulated serotonin overflow with high-K^+ pulses as short as 1 min when determined with 2-min dialysate sampling in ventral striatum. Stimulated serotonin levels in female mice during the high estrogen period of the estrous cycle were similar to serotonin levels in male mice. By contrast, stimulated serotonin overflow during the low estrogen period in female mice was increased to levels similar to those in male mice with local serotonin transporter (SERT) inhibition. Stimulated serotonin levels in mice with constitutive loss of SERT were considerably higher yet, pointing to neuroadaptive potentiation of serotonin release. When combined with brief K^+ stimulation, fast microdialysis reveals dynamic changes in extracellular serotonin levels associated with normal hormonal cycles and pharmacologic vs genetic loss of SERT function.

KEYWORDS: *Mice, sex difference, serotonin transporter, escitalopram, K^+-stimulated overflow*

Serotonin is a neurotransmitter of importance in emotion- and reward-related behavior, as well as related neuropsychiatric disorders and their treatment.[1] *In vivo* microdialysis has been effectively employed to understand pharmacologic,[2−4] genetic,[5−7] and environmental[8−10] impacts on brain serotonin transmission. High temporal resolution in microdialysis sampling enables physiologically important signaling to be investigated and has been developed for glutamate,[11] acetylcholine,[12] and dopamine,[13] among other neurotransmitters and metabolites. However, typical serotonin microdialysis sampling *in vivo* is on the order of 10−30 min.[2−7,10] When coupled with offline analysis, resolution as high as 2 min has been achieved for serotonin sampling.[14−18] Offline approaches often involve decreased throughput, however, due to longer analysis times. Sample degradation and small-volume handling present further challenges. Moreover, offline dialysis does not provide feedback for adjustments during an experiment or facile synchronization of neurotransmitter measurements with behavioral events.

We recently demonstrated improvements in the temporal resolution of online serotonin microdialysis in behaving animals. Using commercially available high-performance liquid chromatography (HPLC) instrumentation, we achieved analysis times for serotonin, which must match online sampling times, as short as 2 min.[19] Furthermore, dialysate serotonin has been resolved in less than 1 min using ultra-high-pressure and temperature capillary separations on a custom instrument.[20−22]

Changes in serotonin levels during microdialysis can be behaviorally evoked[10] or externally stimulated.[23] Reverse dialysis of high-K^+ artificial cerebrospinal fluid (aCSF) has been employed since the 1980s as another means to produce local neurotransmitter release. Durations of high-K^+ stimuli are

Special Issue: Serotonin Research

Received: May 7, 2015
Revised: July 10, 2015
Published: July 13, 2015

DOI: 10.1021/acschemneuro.5b00132
ACS Chem. Neurosci. 2015, 6, 1487−1501

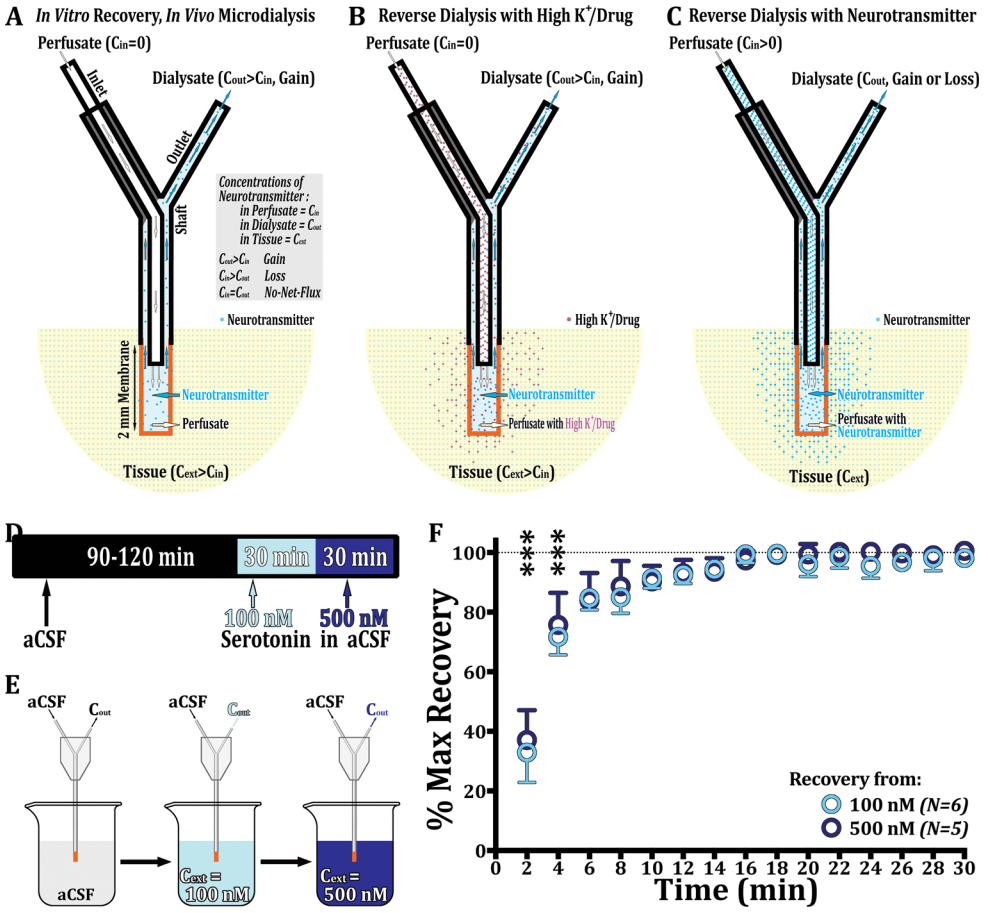

Figure 1. Schematics of different versions of microdialysis experiments and *in vitro* probe performance. In (A), the perfusate is composed of regular artificial cerebrospinal fluid (aCSF). Neurotransmitter molecules diffuse across the membrane in an inward direction during *in vitro* or *in vivo* experiments. In (B), stimulatory concentrations of K^+ (120 mM) and/or a drug (e.g., escitalopram) are included in the aCSF perfusate. High K^+ and drug diffuse down their concentration gradients into the tissue surrounding the probe, whereas neurotransmitter diffuses into the probe from the tissue. In (C), exogenous neurotransmitter is included in the perfusate. The net direction of diffusion is governed by the neurotransmitter concentration difference between the perfusate and tissue. (D) Timeframe and (E) schematic for the *in vitro* probe recovery experiment. (F) Time course data for *in vitro* probe recovery. ***$P < 0.001$ vs 100% recovery.

typically on the order of sampling times.[5,24−29] However, we have shown that undersampling (i.e., sampling times much longer than physiological events), which likely occurs with prolonged high-K^+ perfusion, obscures biologically meaningful information.[19] Here, we determined the high-K^+ pulse durations needed to produce detectable vs maximal serotonin levels in conjunction with fast 2 min online sampling and analysis. We systematically varied short, reverse-dialysis high-K^+ pulse lengths from 1 to 6 min. Repeated maximally evoked serotonin was used to discriminate interstimulus intervals associated with depletion of releasable neurotransmitter.

The National Institutes of Health recently mandated that preclinical research address both sexes.[30] We compared basal and stimulated serotonin levels in female and male mice during their normal reproductive periods. Female mice were divided into two broad estrous phases (metestrus/diestrus vs proestrus/estrus) to consider the influence of regular hormonal variations on brain extracellular serotonin levels. Furthermore, we used fast online microdialysis to investigate whether genetically induced differences in SERT expression are associated with neuroadaptive changes in serotonin release[5,19] by comparing constitutive loss of SERT[31] with acute pharmacologic inhibition of SERT. We find that brief K^+ stimulation evokes serotonin levels that are sensitive indicators of biologically relevant differences in serotonin transmission associated with sex, estrous phase, and mode of SERT inhibition. Fast online microdialysis sampling, in conjunction with the temporally resolved local stimulus paradigm developed here, will be useful for observing, and possibly controlling, rapid, real-time changes in *in vivo* neurotransmission associated with behavioral events, which typically occur on time scales of seconds to minutes.

1. RESULTS AND DISCUSSION

1.1. Microdialysis Probe Performance. Probe recovery and dynamics can be limiting factors under fast microdialysis conditions. We investigated these properties *in vitro* via rapid stepwise increases in serotonin outside of microdialysis probes (Figure 1A,D,E). Dead volumes in the inlet and outlet flow paths were measured, and tubing lengths were adjusted to synchronize inlet solution switching and sample collection (Figure S1, Supporting Information). All measurements were based on time zero being when inlet high serotonin concentrations or high-K^+ pulses reached the probe tips.

In vitro recoveries and response times were determined at two different serotonin concentrations. The lower concentration (100 nM) was selected because it produced dialysate levels comparable to those recovered after maximal K^+-induced

DOI: 10.1021/acschemneuro.5b00132
ACS Chem. Neurosci. 2015, 6, 1487−1501

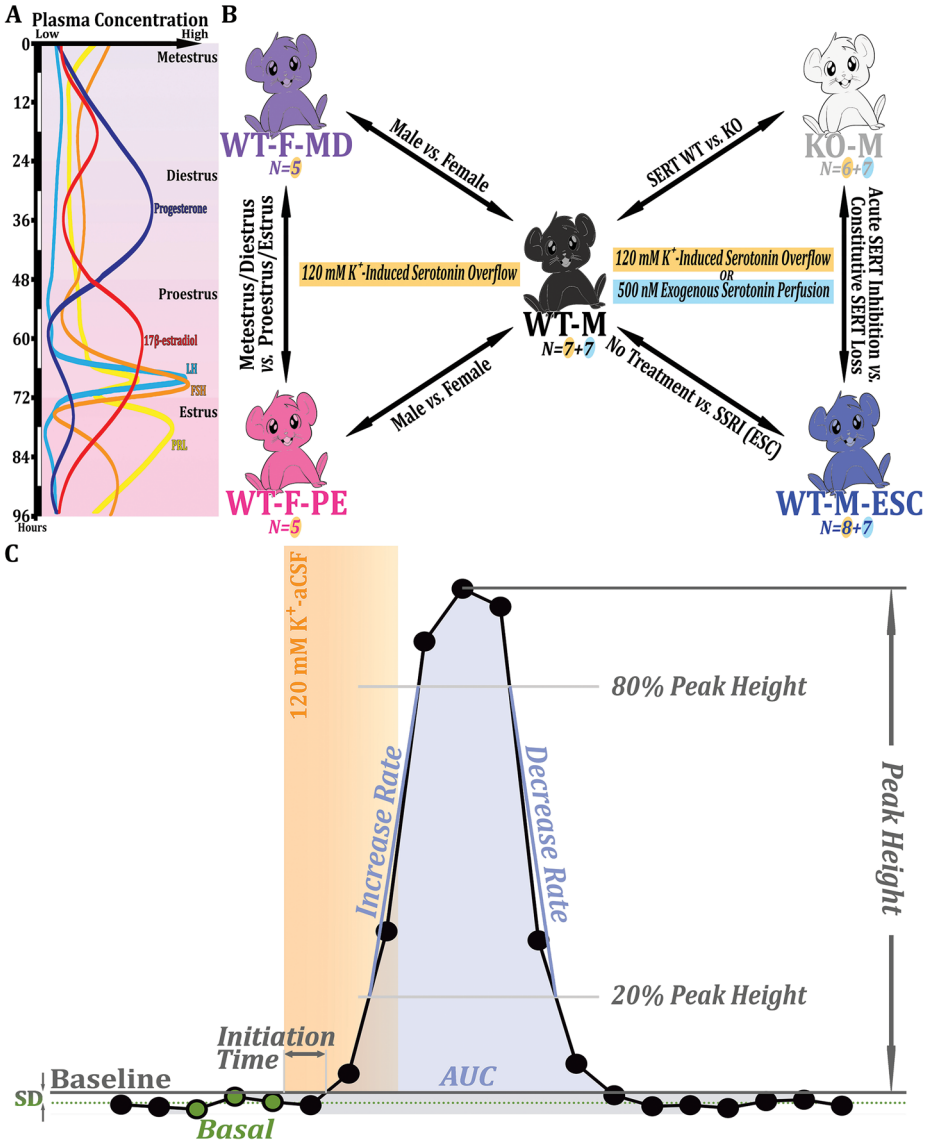

Figure 2. Experimental animal groups and parameter definitions for K^+-induced serotonin overflow peaks. (A) Schematic of the spontaneous rhythms of the major hormones in the estrous cycle in female mice (FSH, follicle stimulating hormone; LH, luteinizing hormone; PRL, prolactin). Adapted with permission from McLean et al.[74] Copyright 2012 Journal of Visualized Experiments. (B) Group numbers in orange correspond to the high-K^+-induced serotonin overflow experiment to examine sex/estrus- and SERT-associated differences in serotonin transmission. Group numbers in blue are from the experiment on tissue-mediated clearance of exogenous serotonin in male mice *in vivo*. (C) Parameter definitions for a hypothetical K^+-induced serotonin overflow peak. In brief, baseline is defined as 1 standard deviation above the measured basal level to exclude the majority of spontaneous basal fluctuations. Baseline is then used to determine the boundaries of the overflow peak. The basal level before each peak is the average of the three samples immediately before the high-K^+ stimulation reaches the brain. Peak height and areas under the curve (AUC) were used to quantify overflow responses. Increase and decrease rates (peak slopes between 20% and 80% of peak height) of each overflow peak are parameters that were hypothesized *a priori* to be related to neurotransmitter release and reuptake rates. However, even with high temporal resolution, increase and decrease rates of change in stimulated serotonin levels were not associated with serotonin release and reuptake rates.

serotonin overflow *in vivo* (*vide infra*). The higher concentration (500 nM) was selected because it yielded dialysate levels representative of those associated with spontaneous circadian-related serotonin surges *in vivo*.[19] Dialysate samples were collected online and analyzed immediately at 2 min intervals.

Maximal *in vitro* relative recoveries ranged from 6 to 14% across different probes. Mean maximal recovery from 100 nM serotonin in aCSF was 9.8 ± 1%. At 500 nM, mean maximal dialysate recovery was 9.3 ± 1%. As such, *in vitro* relative recovery was independent of the serotonin concentrations tested ($t(4) = 0.7$, $P > 0.5$). Sampling every 2 min was sufficient to detect changes in dialysate serotonin as early as the first sample following rapid solution changes (Figure 1F). Maximal dialysate levels were observed within three samples (i.e., 6 min) at both serotonin concentrations investigated. The time to achieve maximal dialysate levels was independent of serotonin concentration ($F_{(1, 9)} = 0.4$, $P > 0.5$; Figure 1F).

These findings suggest that relative recovery is consistent over a range of dialysate serotonin concentrations expected during *in vivo* sampling. Relative recoveries at short sampling times (e.g., 2 min) would be similar to those at longer conventional sampling times (e.g., 20 min) at equal dialysate flow rates. Absolute recovery (fmol serotonin/sample) at short sampling times would be only 10% of the longer sampling time

DOI: 10.1021/acschemneuro.5b00132
ACS Chem. Neurosci. 2015, 6, 1487−1501

absolute recovery due to reduced sample volumes. Regarding speed, while 2 min sampling appears to be fast enough to detect abrupt changes in environmental serotonin, the dynamics of probe dialysate levels (C_{out}) lag behind external concentration changes (C_{ext}).

1.2. Sex- and Estrus-Mediated Differences in Extracellular Serotonin. *1.2.1. Basal Serotonin.* Dialysate serotonin levels in the ventral striatum were compared between wild-type male (WT-M) and female mice. Female animals were divided into proestrus/estrus (WT-F-PE) and metestrus/diestrus (WT-F-MD) groups (Figure 2A,B). Stimulated serotonin levels were analyzed as absolute dialysate concentrations (Figure 3B) and percent basal (%basal) levels (Figure 3C). The latter is a common way to represent microdialysis data to emphasize changes due to high K^+ or other types of perturbations (e.g., pharmacologic, behavioral). However, interpreting neurotransmitter levels as %basal assumes that basal levels are not different across groups. In the case of sex- and estrus-associated effects, basal dialysate serotonin concentrations differed significantly ($F_{(2,42)} = 20$, $P < 0.001$; Figure 4A). In particular, basal serotonin levels were 30% higher in WT-F-MD mice (0.20 ± 0.009 nM) relative to levels in WT-F-PE (0.14 ± 0.005 nM) and WT-M (0.15 ± 0.005 nM) mice.

1.2.2. K^+-Stimulated Serotonin. Reverse dialysis of brief pulses of aCSF containing a stimulatory concentration of high K^+- (120 mM) was used to evoke serotonin release (Figure 1B). Preliminary experiments with 70 mM K^+ indicated that this concentration was insufficient to produce reliable overflow at short pulse durations. The stimulation time course was broadly divided into three epochs. In the first epoch, a series of 1−5 min single high-K^+ pulses with 1 min increases per pulse was delivered with 20 or 21 min interstimulus intervals to investigate the effects of high-K^+ pulse duration on serotonin overflow (epoch I; Figure 3A). After a 53 min recovery period, three 6 min high-K^+ pulses were delivered with 54 min interstimulus intervals to study repeated responses to maximal stimulation (epoch II). Following a 24 min recovery period, another series of three 6 min pulses was applied to investigate a reduced 24 min interstimulus interval (epoch III). We selected 6 min as the longest high-K^+ pulse because preliminary data suggested that mice, regardless of sex or genotype, showed sustained responses to this stimulus duration with 60 min recovery intervals. By contrast, longer high-K^+ perfusions produced diminishing responses after repeated stimulation. To compare responses between groups in epochs I and III, we applied a generalized linear mixed model (GLMM), a statistical method designed to investigate repeated measures correlations allowing for fixed and time-varying covariates. Explanations of these descriptive statistics are in Figure S2.

In addition to the time course of stimulated serotonin overflow (Figure 3B,C), graphs of individual serotonin overflow peaks are depicted at high resolution in Figure S3. A number of parameters describing various aspects of each stimulated overflow peak were calculated (Figure 2C; detailed descriptions in Methods). The parameter most commonly used to assess stimulated microdialysis data is area under the curve (AUC).[3,7,17,29,32] High-K^+-induced serotonin overflow peak heights and slopes were also analyzed.[33−39]

1.2.2.1. Increasing Durations of K^+ Stimulation (Epoch I). Sensitivity to K^+ stimulation was qualitatively assessed by the number of responders per stimulus and initiation time. Serotonin overflow in response to the shortest 1 min high-K^+ pulse was detected in all WT-M subjects, whereas 4/5 mice in both the WT-F-PE and WT-F-MD groups exhibited detectable serotonin overflow. (See Methods for a detailed definition of detectable overflow.) The 2 min high-K^+ pulse elicited detectable overflow in all animals except one male mouse whose prestimulus serotonin level showed an unusually high increase (170%) compared to its level prior to the 1 min K^+ stimulation. All mice responded to all subsequent stimuli. Initiation times showed no significant differences across groups (Figure 4B, Table S1).

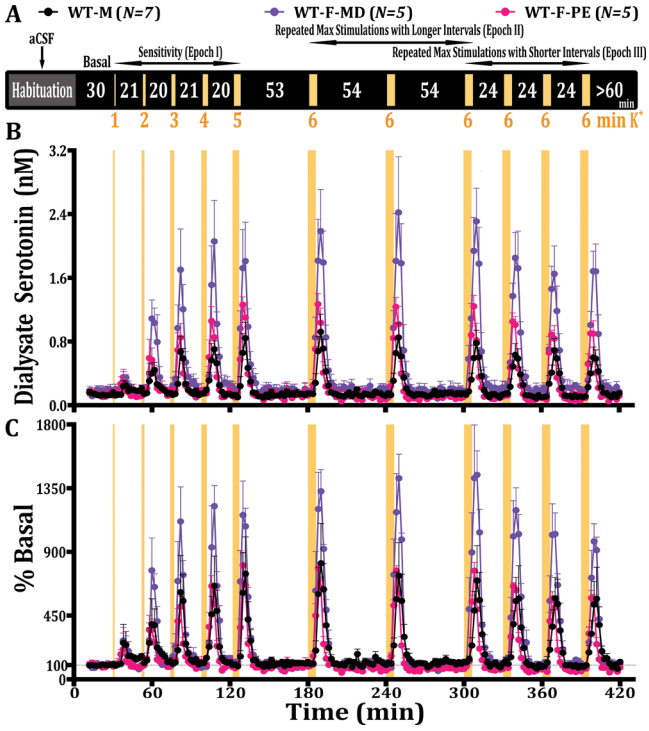

Figure 3. Sex- and estrus-associated differences in basal and stimulated serotonin overflow. (A) Paradigm to investigate differences in sensitivity and response characteristics to repeated high-K^+ pulses in wild-type male (WT-M), wild-type female metestrus/diestrus (WT-F-MD), and wild-type female proestrus/estrus (WT-F-PE) groups. Interstimulus intervals (min) are indicated on the black bar. Stimulation pulse lengths (min) are indicated below in orange. Basal and K^+-induced extracellular serotonin overflow with respect to time (min) are represented as (B) absolute serotonin concentrations and (C) %basal levels.

Response magnitudes to high-K^+ stimulation were characterized by peak heights and AUCs. Increasing stimulus durations evoked greater serotonin overflow (Figures 3B,C and S1). Compared to WT-M mice, WT-F-MD mice showed a greater rate of increase (group × linear stimulus duration interaction $t_{(62)} = 4.7$, $P < 0.0001$) and a concave pattern (group × quadratic stimulus duration interaction $t_{(62)} = -4.1$, $P < 0.001$) in the peak height response trajectory in epoch I (Figure 4C). Responses in epoch I for WT-F-MD vs WT-F-PE groups for peak heights, and among all three groups for AUCs were characterized by similar patterns (Figures 4C,D) and statistics (Tables S2 and S3). Mean outcomes increased linearly for WT-M and WT-F-PE groups. By contrast, mean outcomes for peak heights, and AUCs in the WT-F-MD group showed a linear increase only until the 3 min high-K^+ pulse, after which response magnitudes were maximal and stable.

Ascending and descending overflow peak slopes were used to assess rates of change of extracellular serotonin levels in

DOI: 10.1021/acschemneuro.5b00132
ACS Chem. Neurosci. 2015, 6, 1487−1501

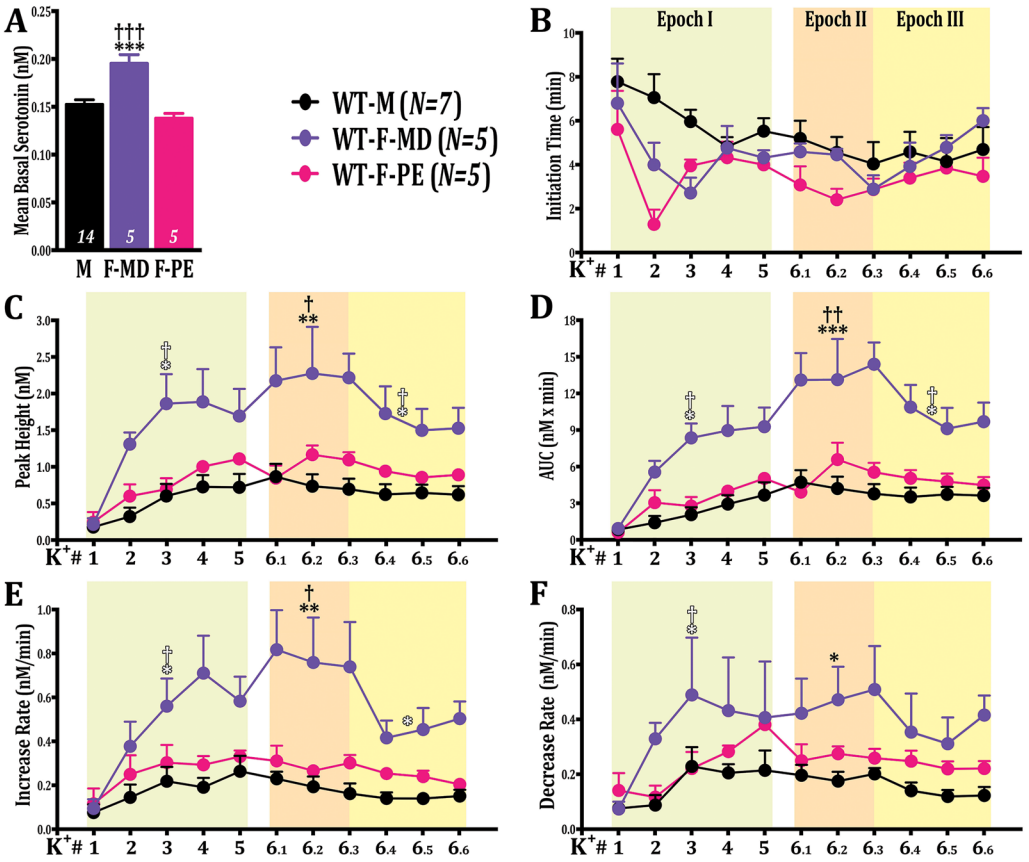

Figure 4. Detailed comparisons of sex- and estrus-associated differences in basal and K^+-induced serotonin overflow. (A) Female mice during the metestrus/diestrus period (F-MD) showed higher basal levels of serotonin compared to those of female mice during the proestrus/estrus period (F-PE) and male mice (M). Basal serotonin levels in wild-type male mice during the K^+ stimulation and exogenous serotonin perfusion experiments were combined; group sizes are depicted at the bottom of each bar. (B) Initiation times in female and male mice. (C) Female mice during metestrus/diestrus (WT-F-MD) exhibited greater responses to K^+ stimulation, as shown by peak heights and (D) areas under the curve (AUC) compared to those of WT-F-PE and WT-M mice. Correspondingly, only WT-F-MD mice showed diminishing serotonin overflow with respect to maximal stimulation at shorter interstimulus intervals. (E) WT-F-MD subjects also exhibited greater increase rates and (F) decrease rates relative to WT-F-PE and WT-M mice. Solid $^*P < 0.05$, $^{**}P < 0.01$, and $^{***}P < 0.001$ vs male mice by two-way ANOVA. Solid $^{\dagger}P < 0.05$ and $^{\dagger\dagger}P < 0.01$ WT-F-PE vs WT-F-MD mice by two-way ANOVA. Open * indicates significant differences vs male mice by generalized linear mixed model (GLMM). Open † indicates significant differences between WT-F-PE and WT-F-MD mice by GLMM.

response to K^+ stimulation. Relative to the WT-M group, ascending slopes in the WT-F-MD group increased more quickly (group × linear stimulus duration interaction $t_{(62)} = 3.0$, $P < 0.01$), exhibiting a modestly concave pattern (group × quadratic stimulus duration interaction $t_{(62)} = -2.4$, $P < 0.05$) with respect to stimulus duration in epoch I (Figure 4E). Longitudinal trajectories for descending slopes for all groups, and with respect to the WT-F-PE group for ascending and descending peak slopes showed patterns (Figure 4E,F) and statistical significances (Tables S4 and S5) that were generally similar to those for peak heights and AUCs.

1.2.2.2. Repeated Maximal K^+ Stimulation with Different Recovery Intervals (Epochs II & III). Repeated 6 min high-K^+ pulses delivered with a longer recovery interval (54 min) elicited stable responses across groups (Figure 3B,C and S1). During epoch II, the WT-F-MD group continued to exhibit larger peak heights ($F_{(2,14)} = 8.9$, $P < 0.01$) and AUCs ($F_{(2,14)} = 15$, $P < 0.001$) compared to those of the WT-F-PE and WT-M groups (Figure 4C,D, Tables S7 and S8), as well as greater increase rates ($F_{(2,14)} = 8.9$, $P < 0.01$) and decrease rates ($F_{(2,14)} = 4.0$, $P < 0.05$) (Figure 4E,F, Tables S9 and S10). Three 6 min high-K^+ stimulations with reduced interstimulus intervals (24 min) were then delivered. In epoch III, the WT-F-MD group again responded with larger response magnitudes compared to those of the WT-F-MD and WT-F-PE groups (Figures 3B,C and S1). Notably, the WT-F-MD group displayed a decreasing longitudinal trajectory for peak heights (group × linear stimulus number interaction $t_{(48)} = -4.1$, $P < 0.001$) and AUCs (group × linear stimulus number interaction $t_{(48)} = -4.5$, $P < 0.001$) compared to trajectories for the WT-M group (Figure 4C,D, Tables S12 and 13). The response magnitude trajectories for the WT-F-MD group were also different from the WT-F-PE group in epoch III. These findings show that sustained responses to repeated maximal high-K^+ pulses at a shorter interstimulus interval occur only in groups with lower magnitude responses (i.e., WT-M and WT-F-PE).

1.3. Acute vs Constitutive Loss of SERT Function. *1.3.1. Basal Serotonin Levels.* We compared mice with genetic loss of SERT (SERT knockout mice; KO-M) to wild-type mice with local, acute SERT inhibition (WT-M-ESC; Figure 2B).[40,41]

Similar to previous results in hippocampus,[19] elevated and stable serotonin levels were observed after continuous reverse dialysis of ESC (1.2 μM) into ventral striatum (Figure 5A). Basal serotonin concentrations were significantly different across groups ($F_{(2,42)} = 380$, $P < 0.001$; Figures 5B and 6A), being higher in KO-M mice (0.91 ± 0.02 nM) and WT-M-ESC

DOI: 10.1021/acschemneuro.5b00132
ACS Chem. Neurosci. 2015, 6, 1487−1501

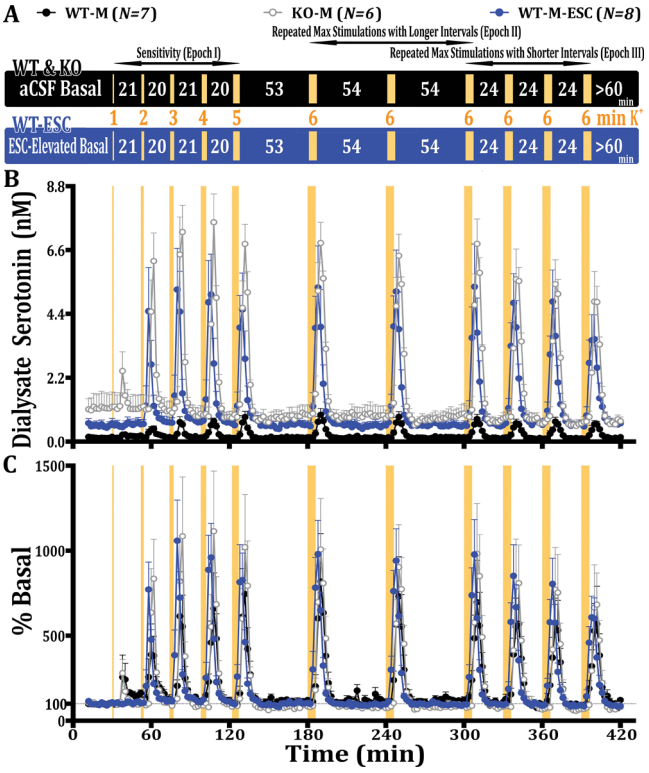

Figure 5. SERT-associated differences in basal and stimulated serotonin overflow. (A) Paradigm for brief 120 mM K^+ stimulus applications used to investigate differences in sensitivity and response characteristics among wild-type male mice (WT-M), male mice with local inhibition of SERT via escitalopram perfusion (WT-M-ESC), and male mice constitutively lacking SERT (KO-M). Interstimulus intervals (min) are indicated on the black and blue bars. Stimulus pulse lengths (min) are indicated in orange. Basal and K^+-induced extracellular serotonin overflow with respect to time are presented as (B) absolute serotonin concentrations and (C) %basal levels.

mice during ESC perfusion (0.67 ± 0.02 nM) than in WT-M mice (0.15 ± 0.005 nM).

1.3.2. SERT Function Modulates K^+-Stimulated Serotonin Overflow. We have long sought to determine whether constitutive loss of SERT is associated with neuroadaptive changes in endogenous serotonin release. Here, we used fast microdialysis with the brief high-K^+ stimulus-pulse paradigm developed above to explore this idea. Stimulated serotonin levels with respect to reduced SERT function were evaluated as absolute dialysate serotonin concentrations and %basal levels (Figure 5B,C). High resolution graphs of individual serotonin overflow peaks for are shown in Figure S4. Here, the two analytical approaches did not lead to similar conclusions. Throughout the K^+ stimulation time course, absolute serotonin levels differed considerably with respect to group (Figure 5B). By contrast, %basal responses were comparable across groups (Figure 5C) due to normalization to highly different basal serotonin levels.

1.3.2.1. Increasing Durations of K^+ Stimulation (Epoch I). Regarding stimulus sensitivity, the 1 min high-K^+ pulse elicited detectable responses in 5/6 KO-M mice (80%), whereas only 3/8 WT-M-ESC mice (40%) showed detectable responses to this pulse. The low number of WT-M-ESC responders to 1 min stimulation suggests that inhibition of SERT restricted to serotonergic terminals increases the threshold for evoked serotonin overflow. Stimulated serotonin was detected in all subjects from the WT-M, WT-M-ESC, and KO-M groups in response to all subsequent stimulations.

Local inhibition of SERT resulted in shorter initiation times in the WT-M-ESC group (Figure 6B). This group displayed a decline in its trajectory of initiation times with respect to stimulus duration (group × linear stimulus duration interaction $t_{(78)} = -3.1$, $P < 0.01$) and a convex curvature of the response trajectory (group × quadratic stimulus duration interaction $t_{(78)} = 2.7$, $P < 0.01$) compared to the WT-M group (Table S16). Differences between WT-M-ESC and KO-M groups were along the same lines. Shorter initiation times in WT-M-ESC mice could reflect faster tissue diffusion of K^+ and/or serotonin. Alternately, serotonin terminals might be more responsive in this group (e.g., decreased resting membrane potential). The latter seems to be at odds with the reduced number of WT-M-ESC responders at the shortest stimulus length. Unfortunately, these and other possibilities cannot be distinguished under the current experimental conditions.

All groups displayed increasing response magnitudes associated with K^+ stimuli of longer durations yet with dissimilar absolute responses across groups (Figures 5B,C and S2). The KO-M group exhibited a greater rate of increase (group × linear stimulus duration interaction $t_{(78)} = 9.3$, $P < 0.001$) and a concave pattern (group × quadratic stimulus duration interaction $t_{(78)} = -7.9$, $P < 0.001$) of longitudinal peak heights vs the WT-M group in epoch I (Figure 6C, Table S17). The WT-M-ESC group showed similar differences in peak height response trajectory vs the WT-M group. Differential group-related patterns were similar for AUCs (Figure 6D, Table S18). In contrast to WT-M mice, KO-M and WT-M-ESC mice reached their maximal peak heights and AUCs at the 3 or 4 min stimulus pulse, respectively. Beyond this, KO-M and WT-M-ESC groups differed from each other in rates of increase (group × linear stimulus duration interaction $t_{(78)} = -5.9$, $P < 0.001$) and concave patterns (group × quadratic stimulus duration interaction $t_{(78)} = 4.9$, $P < 0.001$) associated with peak height trajectories (Figure 6C, Table S17). Differential response trajectories for AUCs were also noted between these two groups (Figure 6D, Table S18).

Relative to peak slopes for WT-M mice, KO-M mice showed a greater increase in ascending peak slopes (group × linear stimulus duration interaction $t_{(78)} = 6.1$, $P < 0.001$) characterized by a highly concave pattern (group × quadratic stimulus duration interaction $t_{(78)} = -5.6$, $P < 0.001$) in epoch I (Figure 6E, Table S19). Similar patterns for increase rates in the WT-M-ESC vs WT-M groups were noted, as were group-related patterns for decrease rates (Figure 6F, Table S20). Maximal serotonin increase and decrease rates were achieved by the 3 min stimulation in all groups; however, rates of change in extracellular serotonin levels then appeared to decrease at the 4 and 5 min stimulations in the WT-M-ESC and KO-M groups relative to the WT-M group (Figure 6E,F). Larger overall descending peak slopes in the KO-M group suggest that alternate clearance mechanisms might be activated at high levels of stimulated release to compensate for loss of SERT function.[42−44] However, the mesoscale temporal resolution employed here (i.e., 2 min sampling is intermediate to conventional dialysis sampling (15−30 min)[2,3,5,7] vs voltammetry sampling (1−10 Hz)[36,45]) is probably insufficient to differentiate release and reuptake processes.

1.3.2.2. Repeated Maximal K^+ Stimulation with Different Recovery Intervals (Epochs II and III). Repeated 6 min stimulations with longer recovery intervals (54 min) were

DOI: 10.1021/acschemneuro.5b00132
ACS Chem. Neurosci. 2015, 6, 1487−1501

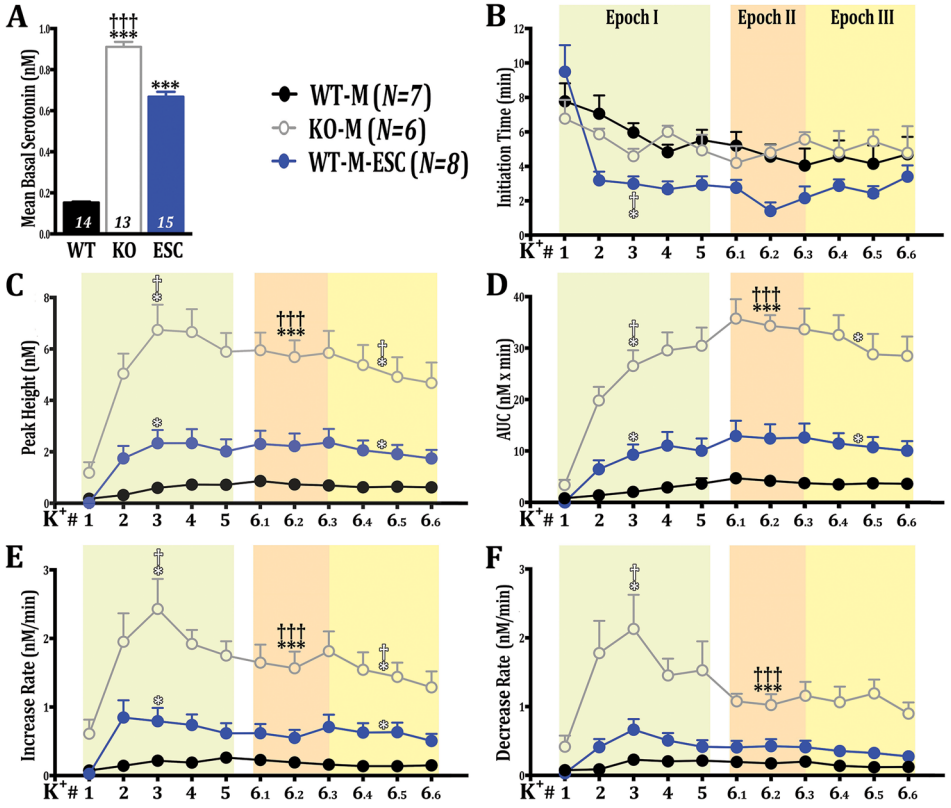

Figure 6. Detailed comparisons of SERT-associated differences in basal and K^+-induced serotonin overflow. (A) Male mice with constitutive loss of SERT (KO) exhibited higher basal serotonin concentrations compared to those in wild-type mice (WT) or wild-type mice with local SERT inhibition due to reverse dialysis of escitalopram (ESC). Basal serotonin levels for WT mice from both the K^+ stimulation and exogenous serotonin perfusion experiments were combined; group sizes are shown at the bottom of each bar. (B) The WT-M-ESC group showed shorter initiation times. Mice lacking SERT (KO-M) exhibited the largest responses to K^+ stimulation in terms of (C) peak height and (D) area under the curve (AUC). The WT-M-ESC group showed moderately enhanced response amplitudes compared to those of WT-M mice. Both the KO-M and WT-M-ESC groups exhibited diminishing responses with respect to maximal (6 min) stimuli when accompanied by a shorter interstimulus interval. The KO-M group had much higher (E) increase rates and (F) decrease rates compared to those of the other two groups. In some cases, increase and decrease rates were also higher in the ESC group compared to the WT group. Solid ***$P < 0.001$ vs WT-M mice by two-way ANOVA. Solid $^{\dagger\dagger\dagger}P < 0.001$ WT-M-ESC vs KO-M mice by two-way ANOVA. Open * indicates significant differences vs WT-M mice by generalized linear mixed model (GLMM). Open † indicates significant differences between WT-M-ESC and KO-M mice by GLMM.

associated with stable responses in WT-M-ESC and KO-M groups. Similar to epoch I, responses in epoch II were significantly different across groups with respect to peak heights ($F_{(2,18)} = 26$, $P < 0.001$) and AUCs ($F_{(2,18)} = 38$, $P < 0.001$) (Figure 6C,D, Tables S22 and S23). The KO-M group exhibited consistently larger response magnitudes relative to the WT-M and WT-M-ESC groups, whereas the WT-M-ESC group showed peak heights and AUCs intermediate to both groups. Repeated 6 min stimuli with reduced recovery intervals (24 min) resulted in diminished serotonin overflow in both the KO-M and WT-M-ESC groups vs the WT-M group, as evidenced by decreasing peak heights (Figure 6C) and AUCs (Figure 6D) during epoch III. For example, peak height responses showed a linear decrease in the KO-M group compared to those of the WT-M group (group × linear stimulus number interaction $t_{(57)} = -7.1$, $P < 0.001$). Comparisons were similar between WT-M-ESC and WT-M groups (Table S27) and for AUCs (Table S28). As in earlier epochs, response magnitude trajectories in epoch III were also different between KO-M and WT-M-ESC groups (Table S27).

1.4. SERT Mediates Exogenous Serotonin Clearance. A final experiment was conducted to dissociate serotonin clearance from release mechanisms *in vivo*. Instead of stimulating endogenous serotonin release, serotonin was delivered to the ventral striatum via reverse dialysis in WT-M, WT-M-ESC, and KO-M mice (Figures 1C and 2B). Local perfusion of 1.2 μM ESC inhibited SERT prior to and during perfusion with 500 nM serotonin in the WT-M-ESC group (Figure 7A). A number of parameters were calculated to describe the behavior of dialysate serotonin levels in response to serotonin perfusion (Figure 7B; detailed descriptions in Methods).

Active uptake of serotonin by SERT appeared to influence the rate at which stable elevated serotonin dialysate concentrations (C_{out}) were established, as suggested by significant differences in ascending half-times ($F_{(2,17)} = 8.1$, $P < 0.01$, Figure 7D). By contrast, ascending slopes (increase rates) were not significantly different across groups ($F_{(2,17)} = 0.59$, $P > 0.5$, Figure 7E), arguing that half-time, as opposed to slope, is a more sensitive indicator of the time needed to reach maximal C_{out}.

Similar to the *in vitro* probe recovery experiments described above, within 6 min of continuous serotonin perfusion *in vivo*, all groups established stable, yet different, dialysate serotonin concentrations ($F_{(2,42)} = 470$, $P < 0.001$; Figure 7C,F). Mice with constitutive loss of SERT exhibited the highest dialysate serotonin levels associated with minimal (0.4%) tissue extraction of perfused serotonin ($C_{out} = 498 \pm 1$ nM). Tissue

DOI: 10.1021/acschemneuro.5b00132
ACS Chem. Neurosci. 2015, 6, 1487−1501

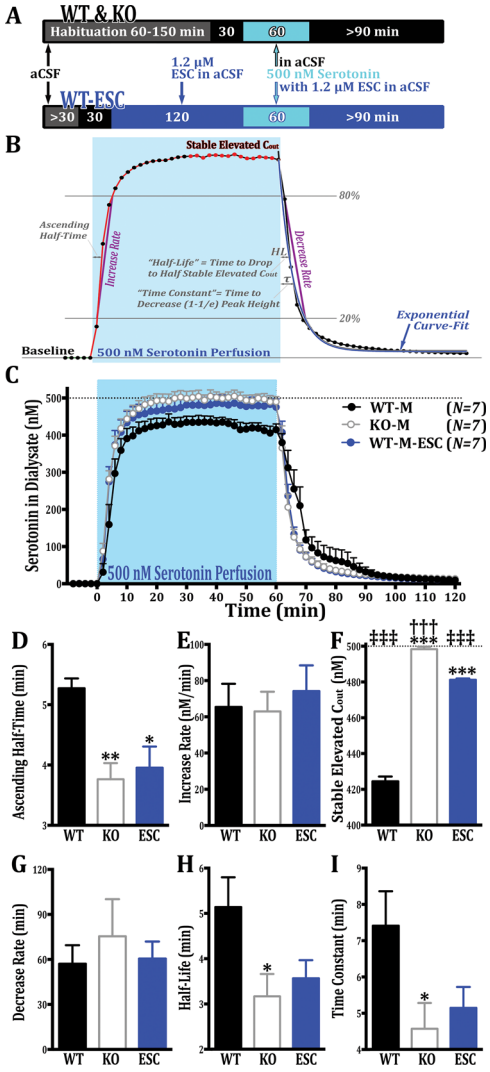

Figure 7. Clearance of exogenous serotonin. (A) Perfusion timelines and (B) parameters. (C) Changes in dialysate serotonin levels with respect to time in response to perfusion of exogenous serotonin. Microdialysis probes were implanted in the ventral striatum in male wild-type mice (WT-M), mice with local inhibition of SERT via escitalopram perfusion (WT-M-ESC), and mice constitutively lacking SERT (KO-M). (D) It took longer for WT-M mice to reach 50% of their stable elevated C_{out} (ascending half-time) relative to KO-M and WT-M-ESC mice during the ascending phase just after beginning perfusion of 500 nM exogenous serotonin, (E) although there were no differences between increase rates *per se*. (F) Stable elevated C_{out} was higher in KO-M mice compared to levels in the other two groups; WT-M-ESC mice showed increased stable elevated C_{out} compared to that in WT-M mice. (G) There were no significant differences in decrease rates. However, the KO-M group exhibited (H) a shorter descending half-life (I) and time constant during the descending phase after exogenous serotonin was removed from the perfusate. $^{*}P < 0.05$, $^{**}P < 0.01$, and $^{***}P < 0.001$ vs WT-M mice. $^{\dagger\dagger\dagger}P < 0.001$ WT-M-ESC vs KO-M mice. $^{\ddagger\ddagger\ddagger}P < 0.001$ vs exogenous serotonin perfusion solution concentration.

extraction was 4% in the WT-M-ESC group and 15% in the WT-M group (C_{out} = 481 ± 1 nM and 424 ± 3 nM, respectively). These findings suggest that in WT-M mice, there is sufficient uptake of serotonin by SERT such that the brain tissue surrounding the probe has the capacity to clear some of the serotonin diffusing from the probe to the tissue during perfusion with 500 nM serotonin. Alternate transporters (e.g., organic cation transporters, dopamine transporters)[43,46] do not appear to compensate appreciably for constitutive loss of SERT under these experimental conditions since in KO-M mice, very little probe serotonin was cleared by the brain tissue.

After 60 min of serotonin perfusion, the dialysis fluid was quickly switched back to aCSF lacking serotonin. All groups showed a rapid drop in C_{out} to basal levels (Figure 7C). Decrease rates were not significantly different across groups ($F_{(2,17)}$ = 0.30, $P > 0.7$; Figure 7C,G). However, visual inspection followed by exponential curve fits of the descending data revealed that KO-M and WT-M-ESC groups exhibited faster recoveries based on descending half-lives ($F_{(2,17)}$ = 3.9, $P < 0.05$) and mean lifetimes (time constants) ($F_{(2,17)}$ = 3.9, $P < 0.05$) (Figure 7H,I).

1.5. General Discussion. Our overarching goal in developing microdialysis methods with high temporal resolution is to enable future studies aimed at uncovering behaviorally relevant information encoded in serotonin signaling. Previously, we showed that faster sampling during online microdialysis improved estimates of basal serotonin levels.[19] Because sampling rates were increased by 10-fold, larger numbers of dialysate samples were collected and analyzed, enabling greater statistical averaging and hence better precision. Furthermore, the overall times needed for basal dialysis and, particularly, no-net-flux estimates of serotonin concentrations were greatly decreased. We showed that improved temporal resolution reduced undersampling, thereby enabling differentiation of brief stress- or circadian-induced increases in endogenous serotonin levels.[19]

In the present study, K^+-stimulated serotonin levels, in addition to basal concentrations, were investigated by fast microdialysis, leading to a number of key findings. Regarding the brief stimulus paradigm used here, we determined that reverse dialysis of high-K^+ pulses as short as 1 min produced detectable serotonin overflow when coupled with 2 min online sampling. In general, serotonin overflow increased with longer stimulus durations. Notably, peak heights and AUCs in the groups of mice with higher stimulation-induced serotonin overflow (i.e., WT-F-MD, WT-M-ESC, KO-M) showed a ceiling effect at longer stimulus durations (Figure 8A,B). Because our experimental design employed a common control group (i.e., the WT-M group; Figure 2B) and siblings were randomly assigned across groups, we were able to compare response magnitudes across all five groups. We found that, with the exception of WT-M vs WT-F-PE and WT-M-ESC vs WT-F-MD groups, all other group comparisons were statistically significant during epoch I with respect to linear and quadratic interactions with group (Figure 8A,B, Tables S31 and S32). As such, the magnitude of the differences between female mice as a function of estrous status was similar to that associated with acute SERT inhibition in male mice. Moreover, the effects of genetic loss of SERT outpaced those observed in any other group.

Mice constitutively lacking SERT showed the largest response to 1 min stimulation (Figure 8A,B). The 2 min stimulation in KO-M mice led to a 5−6-fold increase in serotonin overflow, which did not increase with further increases in K^+ stimulus duration. Thus, KO-M mice are supersensitive to K^+-stimulated endogenous serotonin overflow. Loss of SERT-mediated uptake of serotonin is likely to lead directly to higher stimulated serotonin overflow. Increased serotonin overflow in mice with local inhibition of SERT via reverse dialysis of the SSRI antidepressant (WT-M-ESC)

DOI: 10.1021/acschemneuro.5b00132
ACS Chem. Neurosci. 2015, 6, 1487−1501

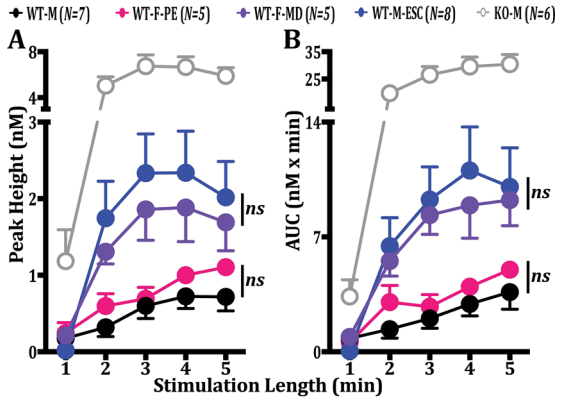

Figure 8. Comparisons of stimulated serotonin overflow across all groups during epoch I. Male mice genetically deficient in SERT (KO-M) showed the highest levels of stimulated serotonin overflow determined by (A) peak heights and (B) areas under the curve (AUC) even at the shortest 1 min stimulation. The KO-M group reached maximal response at the 2 min stimulation. The WT-M-ESC and WT-F-MD groups exhibited moderately elevated responses across the 1−5 min stimuli. Significant differences were detected among all pairwise group comparisons (GLMM) with the exceptions of WT-M-ESC vs WT-F-MD groups and WT-F-PE vs WT-M groups. The latter two groups showed the lowest overall response levels and the greatest stimulus-duration dependence.

substantiates this idea. However, because stimulated overflow was much greater in KO-M mice compared to WT-M-ESC mice, factors beyond loss of SERT function must be at work in the former.

Previous experiments to determine an effective perfusion concentration of ESC indicated that concentrations >1.2 μM did not result in additional increases in basal dialysate serotonin levels.[19] Thus, differences between KO-M and WT-M-ESC groups are not due to incomplete inhibition of SERT in the latter. Neuroadaptive desensitization of serotonin$_{1A}$ autoreceptors in KO-M mice occurs.[47] This prevents autoinhibitory dampening of serotonin release and could lead to higher basal and stimulated dialysate serotonin levels in KO-M mice. By contrast, in WT-M-ESC mice, SERT inhibition is limited to striatal serotonergic terminals; somatodendritic SERT and serotonin$_{1A}$ autoreceptors in the raphe presumably function normally.

Serotonin synthesis rates are increased in mice constitutively lacking SERT.[48] We hypothesized that increased synthesis occurs in response to the loss of the recycled pool of intracellular serotonin in SERT-deficient mice, reflected by 60−80% reductions in brain tissue serotonin levels.[31,48] Increased synthesis could contribute to an increase in the readily releasable pool of serotonin; this pool is known to be sensitive to changes in uptake and synthesis.[49] Although the current study does not provide direct evidence for differences in serotonin release *per se*, we hypothesize that presynaptic serotonin$_{1A}$ autoreceptor desensitization/downregulation,[47,50] in conjunction with increased synthesis,[48] could underlie greater evoked serotonin overflow in KO-M vs WT-M and WT-M-ESC groups.

Mice genetically lacking SERT were previously discovered to show a loss of frequency-dependent serotonin release when brain slices containing the substantia nigra were investigated by FSCV.[51] The authors concluded that abolishing SERT leads to a large summation of extracellular serotonin regardless of stimulus strength. The time scales are different for stimulation and recording in FSCV or fast microdialysis. Nonetheless, loss of normal responses to stimuli of increasing strength (i.e., electrical pulse frequency for FSCV or high-K+ duration for microdialysis) in SERT knockout mice appears to be observed in both experimental paradigms. The similarity of these findings increase support for the notion that behavioral alterations in mice lacking SERT might arise from dysfunctional neurotransmission associated with poor stimulus sensitivity.[51]

When subjected to repeated 6 min K^+ stimuli in combination with a longer interstimulus recovery interval (epoch II), all groups of mice showed reproducible, nondecrementing serotonin overflow (Figures 3B,C and 5B,C). Notably, groups of mice with the highest levels of stimulated serotonin overflow, namely, the WT-F-MD, WT-M-ESC, and KO-M groups, showed diminishing responses to repeated 6 min stimuli when a shorter interstimulus interval was applied (epoch III). This suggests some loss of the readily releasable pool of serotonin under conditions of greater and more frequent stimulated serotonin release. Alternately, these effects could be due to circuit adaptations involving other neurotransmitters, plasticity, or alterations in autoreceptor function. Overall, the brief high-K^+ stimulus paradigm used here, which includes sequential application of stimuli with increasing lengths followed by maximal stimuli at different interstimulus intervals, maps a range of serotonin overflow responses such that sex-, pharmacologic-, and genotype-related influences on serotonin transmission are readily differentiated. Multistimulus paradigms have been used in electrophysiology and FSCV but are enabled only in microdialysis when sampling times are short.

Another important finding that emerges from the present data is that basal and stimulated serotonin levels vary in the ventral striatum across estrous periods in female mice. In rodents, the estrus phase is immediately preceded by proestrus. Proestrus and estrus are together referred to as the follicular phase in women. Estrogen levels surge just prior to ovulation in female mammals, which typically occurs at the end of estrous phase (Figure 2A). Metestrus and diestrus follow ovulation sequentially in rodents; in women, the corresponding period is the luteal phase. In the present study, we observed that basal and stimulated serotonin levels were higher in WT-F-MD mice during the lower estrogen period in mice. Conversely, stimulated serotonin levels were lower in WT-F-PE mice, corresponding to the higher estrogen period. These findings suggest an inverse relationship between estrogen levels and serotonin transmission. We were unable to identify previously published microdialysis studies on estrus-related variations in brain extracellular serotonin levels in mice. However, similar to the present findings, extracellular serotonin levels were higher in the hypothalamus of rats during metestrus/diestrus.[52] Decreased SERT function has been associated with lower estrogen levels in nonhuman primates.[53−55] Reduced serotonin uptake during metestrus/diestrus might underlie increased basal and stimulated serotonin in WT-F-MD mice.

Laboratory staff can be readily trained to determine estrous status (see Supporting Information). The procedure requires only a low-power microscope and basic laboratory supplies. Here, we observed robust differences in basal and stimulated serotonin levels between WT-F-MD and WT-F-PE mice using 10 total female mice vs 7 male mice. Normal hormonal-related variations in serotonin transmission in female animals are remarkable in that they are on par with those associated with SSRI-related changes (Figure 8A,B). The effects of many clinically important drugs in females are not known.[56] Thus, it

DOI: 10.1021/acschemneuro.5b00132
ACS Chem. Neurosci. 2015, 6, 1487−1501

will be important to include normally cycling female animals in preclinical studies necessitating only minimally increased female group sizes, in combination with estrous phase determination. This is in lieu of ovarectomizing females and administering known amounts of estrogen, which is not representative of normal hormonal cycling in most reproductive-aged women.

In microdialysis, AUCs have been used to quantify magnitudes of neurotransmitter release. We and others refer to this released component as overflow because neurotransmitter must escape synapses and cellular uptake diffusing through tens to hundreds of micrometers of tissue to reach dialysis probes.[57] Furthermore, in microdialysis, dynamics are influenced by the time needed for depolarizing concentrations of K^+ to reach serotonin neurons during reverse dialysis. Even with higher sampling rates, probe dynamics (Figure 1) and, more so, tissue diffusion somewhat obscure biological dynamics. Therefore, even with 2 min sampling, it is not possible to deconvolute endogenous neurotransmitter release magnitudes and rates from peak heights and ascending overflow peak slopes, respectively.

Similarly, overflow peak decrease rates are not indicative of serotonin clearance rates, even with the fast sampling times used here. We observed that decrease rates were higher in the KO-M group than decrease rates in WT-M-ESC and WT-M mice (Figure 6F). To investigate this further, we perfused serotonin (500 nM) into the ventral striatum to investigate uptake of exogenous serotonin (Figure 7C). The plateau phase during perfusion showed that in mice with acute local SERT inhibition or mice lacking SERT expression there was little to near-zero loss of exogenous serotonin to the tissue, which we found to be somewhat surprising. At this time, we do not have an explanation for why a greater loss of serotonin to the brain tissue in the WT-M-ESC and KO-M groups was not observed in light of the $C_{in} \gg C_{ext}$ concentration gradient and clearance by diffusion. In WT-M mice, the plateau serotonin concentration was significantly lower than the serotonin concentration entering the probe (C_{in}). This strongly suggests that brain tissue surrounding the probes in WT-M mice is actively clearing serotonin (Figure 7F). When decrease rates were examined, they showed the same trends as those observed in the K^+-stimulation experiment (KO-M ≈ WT-M-ESC > WT-M).

Decrease rates, descending half-lives, and time constants did not correlate with SERT function (Figure 7G–I). Thus, these overflow peak parameters cannot be used to assess clearance rates in fast microdialysis like they can in FSCV.[33] There are a number of possible explanations for this observation. First, in WT mice, extraction fraction (*in vivo* recovery), which is sensitive to uptake,[58] may change over the time course of each high-K^+ stimulus pulse as uptake rates change with respect to increasing and decreasing extracellular serotonin levels.[59,60] By contrast, in mice with local SERT inhibition or loss of SERT expression, extraction fraction is likely to remain constant over a stimulus pulse. In the absence of evidence for substantial clearance by alternate transporters, changing/reversing tissue concentration gradients in WT-M mice may contribute to slower increase and decrease rates compared to those measured in KO-M mice (Figure 7H,I).

Alternately, exposure to high levels of extracellular serotonin in wild-type mice during high-K^+ stimulation or exogenous serotonin perfusion could result in greater transported/intracellular serotonin. As extracellular serotonin levels fall after stimulation/perfusion, reverse transport might occur releasing excess serotonin back into the extracellular space, thereby slowing the apparent decrease rates in WT-M mice. Another possibility is that exposure to high levels of extracellular serotonin during stimulation/perfusion might provoke subsequent exocytotic release in WT-M vs WT-M-ESC and KO-M mice. Notably, even at the higher sampling rates used here, we were unable to fit decrease rates to exponential decay curves because of too few sampling points at stimulated overflow peak summits and on the descending arms of the stimulus curves (Figures S1 and S2). In all, it may not be of much value to analyze overflow peak increase and decrease rates in future fast microdialysis studies since these do not appear to be related to serotonin release and reuptake rates, as initially hypothesized.

2. CONCLUSIONS AND FUTURE DIRECTIONS

There are a number of advantages associated with fast microdialysis when it is combined with brief high-K^+ stimulus pulses. Because dialysis sampling can be coupled with different high sensitivity analytical methods, a wide variety of neurotransmitters and neuromodulators can be investigated, and multiplexed,[11,19,61] compared to currently available direct monitoring techniques (e.g., FSCV, biosensors). Moreover, local stimulus and/or drug delivery, in combination with neurotransmitter sampling, occurs via a single device. Importantly, as Sarter and Kim recently opined for the case of acetylcholine, behaviorally relevant information encoded in neurotransmitter/neuromodulator signaling likely occurs over time frames ranging from hundred of milliseconds to minutes.[62] Longer signaling events are well-suited to elucidation using highly temporally resolved online microdialysis in behaving animals.

In conclusion, brief high-K^+ stimulation is beneficial in conjunction with fast online microdialysis sampling to elucidate biologically important differences in serotonin neurotransmission. This is illustrated by the current findings wherein sex, estrous status, and SERT function were shown to modulate sensitivity and response intensity to stimulation. We believe that fast microdialysis will be useful for advancing knowledge about serotonergic encoding of emotionally salient information.

3. METHODS

3.1. Animals. A total of 53 mice underwent microdialysis testing. All mice were generated at the University of California, Los Angeles (UCLA) from a SERT-deficient lineage[31,63,64] on a mixed CD1 × 129S6/SvEv background via SERT wild-type pairings or heterozygous SERT-deficient mouse pairings. Virgin female mice were studied during their prime reproductive period of 3–6 months of age. Male mice were studied during their typical reproductive period of 2–10 months of age. Mice were housed in groups of 4 to 5 same-sex siblings per cage until guide cannula implantation surgery, after which mice were individually housed. Food and water were available *ad libitum*. The light–dark cycle (12/12 h) was set to lights on at 0600 h (ZT0). The same light schedule was strictly maintained in the room where microdialysis was performed. The Association for Assessment and Accreditation of Laboratory Animal Care International has fully accredited UCLA. All animal care and use met the requirements of the NIH Guide for the Care and Use of Laboratory Animals, revised 2011. The UCLA Chancellor's Animal Research Committee (Institutional Animal Care and Use Committee) preapproved all procedures.

We used the following guidelines during this study to reduce animal use and to decrease variability associated with life events (e.g., parenting, nursing, litter effects, etc.) and environmental factors (e.g., time of day, season, etc.) (1) Siblings from the same litter were randomly assigned to different test groups based on gender and genotype, but they were tested in the same cohort. (2) No more than

DOI: 10.1021/acschemneuro.5b00132
ACS Chem. Neurosci. 2015, 6, 1487–1501

three siblings were assigned to the same group. (3) Each test group contained subjects from ≥3 different parent pairs. Female test subjects were from 7 different litters from 7 different parent pairs. (4) Each group contained subjects from both primi- and multiparous mothers. (5) The study included two cohorts tested over the course of 1 year, with each cohort including subjects representing all groups. (6) All subjects were tested at the same time of day.

3.2. High-Performance Liquid Chromatography. Analysis was performed using an Eicom integrated HPLC system (HTEC-500, Eicom Corporation, San Diego, CA) with an Insight autosampler and two Eicom EAS-20s online autoinjectors. Chromatographic separation was achieved using an Eicompak PP-ODS II stationary phase (4.6 mm i.d. × 30 mm, 2 μm particle diameter) and a phosphate buffered mobile phase with 96 mM NaH_2PO_4 (Fluka no. 17844), 3.8 mM Na_2HPO_4 (Fluka no. 71633), pH 5.4, 2−10% MeOH (EMD no. MX0475-1), 50 mg/L EDTA·Na_2 (Fluka no. 03682), and 500−1000 mg/L sodium decanesulfonate (TCI no. I0348) in water purified via a Milli-Q Synthesis A10 system (EMD Millipore Corporation, Billerica, MA). The column temperature was maintained at 20−25 °C. The volumetric flow rate was 450−750 μL/min. Electrochemical detection was performed using an Eicom WE-3G graphite working electrode with an applied potential of +450 mV vs a Ag/AgCl reference electrode.

Serotonin (Sigma no. H9523) standards were prepared in aCSF (147 mM NaCl (Fluka no. 73575), 3.5 mM KCl (Fluka no. 05257), 1.0 mM $CaCl_2$ (Aldrich no. 499609), 1.0 mM NaH_2PO_4, 2.5 mM $NaHCO_3$ (Fluka no. 88208), 1.2 mM $MgCl_2$ (Aldrich no. 449172), pH 7.3 ± 0.03, at room temperature. Standard curves, which were verified daily, encompassed physiological serotonin concentration ranges (0−100 fmol for *in vivo* high-K^+-induced overflow and 0−20 μmol for *in vitro* probe recovery and exogenous serotonin clearance experiments). The limit of detection was ≤160 amol, and the practical limit of quantification was ≤320 amol. All dialysate samples for *in vitro* and *in vivo* experiments were collected at 2 min intervals at a dialysate flow rate of 3 μL/min using online EAS-20s autoinjectors. Samples were injected immediately onto the HPLC system.

3.3. *In Vitro* Probe Recovery. Throughout the study, CMA/7 microdialysis probes (membrane length 2 mm; CMA/Microdialysis, Solna, Sweden) were used. The dead volume of the perfusion tubing prior to and after the probes was measured to correct for the time needed for high-K^+ pulses to reach the dialysis membranes (Figure S1). *In vitro* recovery and membrane dynamics were studied at room temperature in unstirred solutions. In brief, the entire active membrane of each probe was submerged in 10 mL of regular aCSF and perfused at 3 μL/min for 90−120 min. This was followed by 30 min of data collection beginning after rapidly replacing the aCSF solution with 100 nM serotonin in aCSF. Each probe was then quickly transferred to a solution of 500 nM serotonin in aCSF for an additional 30 min. Concentrations of both serotonin solutions were independently verified before and after the 30 min recovery periods via direct injection onto the HPLC system. Changes in the concentrations of these solutions at room temperature over the duration of the experiment were <5%.

Terminologies for serotonin concentrations are defined in Figure 1A−C and follow conventional microdialysis theory.[57,60,65] Here, C_{in} (nM) is defined as the concentration of serotonin in the dialysis solution entering the probes. The concentration of serotonin exiting the probes is termed C_{out} (nM). The concentration of serotonin in the brain tissue surrounding the probes is C_{ext} (nM). The extraction fraction (E_d) is the inverse of *in vivo* probe recovery. Of note, we have not yet incorporated more recent theories regarding the complex nature of E_d and inequalities with *in vivo* recovery.[59,66−68] The variables defined above are related via the no-net-flux equation as follows: $E_d = (C_{out} - C_{in})/(C_{ext} - C_{in})$.

Serotonin concentrations recovered with respect to time for each probe were measured at C_{ext} = 100 and 500 nM. For *in vitro* recovery, C_{out} measured during the last 10 min of the 30 min recovery period for each probe was averaged across samples to determine maximal recovery (nM). The percent recovery (%recovery) for each probe was calculated as the ratio of each probe's maximal recovery (nM)/C_{ext} (nM) × 100%. To determine instantaneous percent maximum (% max) recoveries, C_{out} for each sample was divided by the maximal recovery for the specific probe used ×100%. Instantaneous %max recoveries were normalized to individual probe recoveries to focus on differences over time vs recovery differences across individual probes.

3.4. Guide Cannula Implantation Surgery. Mice were implanted unilaterally with a single guide cannula for a CMA/7 microdialysis probe aimed at the right ventral striatum (coordinates relative to Bregma: AP +1.2 mm, ML +1.2 mm, DV −3.5 mm) under isoflurane anesthesia. The ventral striatum is integral to brain function associated with reward, mood, stress coping, memory, and learning.[69−73] Analgesia was provided by local administration of bupivacaine just prior to incision (3 mg/kg, sc) and systemic ketoprofen (5 mg/kg/day, sc, for 72 h). Each cannula was secured to the skull with dental resin (Bosworth Trim II, Bosworth Company, Skokie, IL) and a stainless steel screw (Eicom-USA, San Diego, CA). Microdialysis experiments described below were performed 3−10 days after cannula implantation. We previously observed that most female mice, regardless of their presurgery estrous status, exhibit (pseudo-) proestrus/estrus phenotypes by vaginal smear within 24 h after surgery that persists for up to 4 days. For this reason, all female subjects were given a minimal 5 day recovery to allow a return to normal estrous cycling prior to performing microdialysis.

3.5. Probe Insertion. At ZT10−12, each subject was briefly (1−3 min) anesthetized using isoflurane for insertion of a CMA/7 microdialysis probe into the guide cannula. Immediately after insertion, regular aCSF was continuously perfused through the probe at 3 μL/min for 30−60 min followed by a 0.3−1.1 μL/min flow rate for an additional 12−14 h to allow recovery from acute neurotransmitter release due to probe insertion.

3.6. High-K^+-Induced Serotonin Overflow. Female and male mice were used in experiments to determine the effects of sex, estrous phase, and SERT function on basal extracellular serotonin levels and K^+-induced serotonin overflow (Figure 2B). For all mice, at ZT0:30−1:00 on the day after probe insertion, the aCSF flow rate through the probes was increased to 3 μL/min for 60−150 min prior to collecting dialysate samples for analysis. Basal samples were collected in 2 min increments over the course of 30 min. Serial 1−6 min infusions of high isosmotic K^+ aCSF (31 mM NaCl, 120 mM KCl, 1.0 mM $CaCl_2$, 1.0 mM NaH_2PO_4, 2.5 mM $NaHCO_3$, 1.2 mM $MgCl_2$, pH 7.3 ± 0.03, at room temperature) were then delivered using a programmable microdialysis infusion pump (CMA/102) with predetermined durations and order (Figure 3A). Stimulation data were divided by design into three epochs (Figures 3 and 5). Epoch I comprised the period associated increasing K^+ stimulation length. Epoch II involved repeated maximal stimulation with a longer interstimulus interval, and epoch III examined repeated responses to maximal stimulations with shorter interstimulus intervals.

For WT-M mice receiving ESC (Figure 5A; BioTrend Chemicals AG, no. BG0433), microdialysis was carried out as described above. Here, basal samples were collected in 2 min increments over the course of 30 min, after which ESC-aCSF (1.2 μM ESC, 147 mM NaCl, 3.5 mM KCl, 1.0 mM $CaCl_2$, 1.0 mM NaH_2PO_4, 2.5 mM $NaHCO_3$, 1.2 mM $MgCl_2$, pH 7.3 ± 0.03, at room temperature) was perfused into the probes for the duration of the experiment. Samples were collected for another 2 h to establish ESC-elevated serotonin concentrations. Subsequently, mice received the high-K^+ stimulus sequence in ESC-aCSF (Figure 5A; 1.2 μM ESC, 31 mM NaCl, 120 mM KCl, 1.0 mM $CaCl_2$, 1.0 mM NaH_2PO_4, 2.5 mM $NaHCO_3$, 1.2 mM $MgCl_2$, pH 7.3 ± 0.03, at room temperature). After the last stimulation, sample collection continued for at least another 60 min for all subjects.

3.7. Exogenous Serotonin Clearance. Male mice were used to investigate the influence of SERT expression and function on serotonin clearance (Figure 7A). For WT-M and KO-M mice, after implantation and overnight equilibration, the aCSF flow rate through the microdialysis probes was increased to 3 μL/min for 60−150 min before collecting dialysate samples. Basal samples were collected in 2 min increments for 30 min. Next aCSF containing serotonin (500 nM serotonin, 147 mM NaCl, 3.5 mM KCl, 1.0 mM $CaCl_2$, 1.0 mM

DOI: 10.1021/acschemneuro.5b00132
ACS Chem. Neurosci. 2015, 6, 1487−1501

NaH_2PO_4, 2.5 mM $NaHCO_3$, 1.2 mM $MgCl_2$, pH 7.3 ± 0.03, at room temperature) was perfused via the microdialysis probes for 60 min. The perfusion solution was then switched back to regular aCSF using CMA/110 liquid switches for at least 90 min. For WT-M-ESC mice, after establishing ESC-elevated serotonin levels, mice were dialyzed with 500 nM exogenous serotonin in ESC-aCSF (500 nM serotonin, 1.2 μM ESC, 31 mM NaCl, 120 mM KCl, 1.0 mM $CaCl_2$, 1.0 mM NaH_2PO_4, 2.5 mM $NaHCO_3$, 1.2 mM $MgCl_2$, pH 7.3 ± 0.03, at room temperature) for 60 min, followed by ESC-aCSF perfusion and sample collection for at least another 90 min. The 500 nM aCSF serotonin solutions used in these experiments were verified before and after perfusion by direct measurement via the HPLC system. Changes in serotonin concentration in perfusates were <5% over the course of the experiment.

3.8. Vaginal Smear. Vaginal smears were analyzed for all female subjects prior to and immediately following microdialysis to assess estrous status.[74] Additional information on this procedure appears in the Supporting Information.

3.9. Probe Verification. After microdialysis experiments, mice were sacrificed by cervical dislocation and their brains were rapidly removed. The anterior portion of each brain including the ventral striatum was fixed in 7% paraformaldehyde phosphate buffer (PB), pH 7.3, for 48−72 h at room temperature on a laboratory rotator. Brains were then transferred to 30% sucrose in phosphate buffer and stored at −80 °C. Fixed brains were sectioned at 50 μm using a cryostat and stained using cresyl violet. Probe locations were verified at 100× magnification.

3.10. Data Analysis. Each K^+-induced serotonin overflow peak was identified and analyzed individually using the following criteria and procedures:

(1) Concentrations of serotonin in three dialysate samples immediately preceding the onset of each stimulation were averaged and denoted as basal serotonin levels (nM; Figure 2C). Basal serotonin levels were detected in all mice.
(2) The baseline (nM) for each overflow peak was defined as basal + 1 standard deviation (SD) to account for spontaneous fluctuations in basal serotonin levels.
(3) The time from the start of each high-K^+ pulse to the time for the dialysate serotonin level to reach baseline was defined as the initiation time (min). In cases of no detectable response, the value of the initiation time was set to 12 min, which was greater than the longest initiation time, and the values of the peak height and AUC were set to zero (see below).
(4) The boundaries of each K^+-induced serotonin overflow peak were determined by continuous dialysate samples containing serotonin levels >baseline. If no dialysate samples contained serotonin levels above baseline, then that stimulus was recorded as provoking no response.
(5) Peak height (nM) was determined by subtracting the baseline level from the highest measured dialysate serotonin level during a stimulus application.
(6) The area under the curve (AUC; nM × min) was determined from the measured area under the concatenated dialysate serotonin samples within the overflow peak. The base of the overflow peak was defined by the baseline.
(7) The increase rate (nM/min) and decrease rate (nM/min) were defined by the slopes of the overflow peak between 20 and 80% of the peak height on the ascending and descending arms, respectively. In cases of no detectable response, the values of both rates were set to zero.

Similarly, each of the following parameters were calculated for the 500 nM perfusion data (Figure 7B):

(1) The average value of the three samples immediately before the switch to 500 nM exogenous serotonin perfusion was defined as basal (nM), and the baseline (nM) was defined as basal + 1 SD.
(2) The average value of dialysate serotonin during the last 30 min of the 500 nM perfusion period was defined as the stable elevated C_{out} (nM).
(3) The increase rate (nM/min) and decrease rate (nM/min) during the perfusion period were defined by the slopes between 20 and 80% of the differences between the stable elevated C_{out} and baseline on the ascending and descending phases.
(4) The time between the onset of perfusion to 50% of the stable elevated C_{out} was defined as the ascending half-time (min).
(5) The data points on the descending phase of the peak were fit to an exponential decay model to calculate descending half-life (min) and time constant (tau; min).

3.11. Statistics. *In vitro* percent maximal recoveries were compared by paired two-tailed Student's *t* tests. Time course data for *in vitro* probe recovery experiments were analyzed by two-way ANOVA with %max recovery (between subjects) and time (within subjects) as the independent variables and *posthoc* Tukey's multiple comparisons.

For K^+ stimulation experiments, data were divided into three epochs based on experimental design (see above). Data from epochs I and III were analyzed using generalized linear mixed models (GLMM). The GLMM procedure accounts for correlations between repeated measures within subjects and allows for both fixed and time-varying covariates. Use of GLMM facilitated the analysis of the complex relationships between the different groups and repeated K^+ stimuli (Figure S2).

For epoch I, the group × linear stimulus duration interactions and the main effects of group and stimulus duration were used to model the longitudinal trajectories of the mean outcomes with respect to increasing K^+ stimulus duration (Figures 4B−F and 6B−F, green boxes). Due to the curvilinear nature of some of the trajectories, we included a quadratic term for stimulus duration in the main effects and interactions with group. For epoch III, longitudinal outcomes associated with maximal K^+ stimulation and shorter interstimulus intervals were also analyzed using GLMM. Here, the data were modeled using group × linear stimulation number interactions, main effects of group, and number of previous stimulations (1 through 4). Initial analysis did not yield evidence for quadratic behavior in these data trajectories; thus, only a linear term was included in the model (Figures 4B−F and 6B−F, yellow boxes).

In epoch II, maximal K^+ stimulation with the longer interstimulus interval was not predicted to have an order effect (i.e., we hypothesized that responses would be similar regardless of stimulus number in this epoch) (Figures 4B−F and 6B−F, orange boxes). Therefore, these data and the remaining between-group comparisons were analyzed by a two-way ANOVA model followed by *posthoc* Tukey's multiple comparisons. Comparisons of peak heights and AUCs across all experimental groups (Figure 8) were analyzed by GLMM as described above for epoch I data.

Statistical analyses were carried out using Prism, v.6f (GraphPad Inc., La Jolla, CA), or SAS, v.9.4 (SAS Institute Inc., Cary, NC). Data are expressed as group means ± SEMs, with $P < 0.05$ considered to be statistically significant. Of the 53 mice studied, one KO-M mouse in the K^+ stimulation experiment was excluded from analysis because of unusually high responses in term of peak heights and AUCs (>4 SDs from the population mean).

■ ASSOCIATED CONTENT

Supporting Information

High-resolution graphs of K^+-induced serotonin overflow peaks, detailed vaginal smear procedures, and statistical tables. The Supporting Information is available free of charge on the ACS Publications website at DOI: 10.1021/acschemneuro.5b00132.

■ AUTHOR INFORMATION

Corresponding Author

*E-mail: aandrews@mednet.ucla.edu. Phone: 310-794-9421.

Author Contributions

The experiments were designed by H.Y. and A.M.A. and carried out by H.Y. with assistance from M.M.S. The statistical analyses

DOI: 10.1021/acschemneuro.5b00132
ACS Chem. Neurosci. 2015, 6, 1487−1501

were designed by D.S. and carried out by H.Y. All authors wrote the manuscript.

Funding

The content is solely the responsibility of the authors and does not necessarily represent the official views of the National Institute of Mental Health or the National Institutes of Health. Support from the National Institute of Mental Health (MH064756, MH086108), the Brain & Behavior Research Foundation (formerly NARSAD), the Shirley and Stefan Hatos Foundation, and the UCLA Weil Endowment Fund are gratefully acknowledged.

Notes

The authors declare the following competing financial interest(s): A.M.A. has received compensation from Forest Laboratories (Actavis) for work as a consultant..

REFERENCES

(1) Altieri, S. C., Singh, Y. S., Sibille, E., and Andrews, A. M. (2012) Serotonergic pathways in depression, in *Neurobiology of Depression* (López-Muñoz, F., and Álamo, C., Eds.) Taylor and Francis Group, Boca Raton, FL.

(2) Sharp, T., Umbers, V., and Gartside, S. E. (1997) Effect of a selective 5-HT reuptake inhibitor in combination with 5-HT1A and 5-HT1B receptor antagonists on extracellular 5-HT in rat frontal cortex in vivo. *Br. J. Pharmacol. 121*, 941−946.

(3) Richardson-Jones, J. W., Craige, C. P., Guiard, B. P., Stephen, A., Metzger, K. L., Kung, H. F., Gardier, A. M., Dranovsky, A., David, D. J., Beck, S. G., Hen, R., and Leonardo, E. D. (2010) 5-HT1A autoreceptor levels determine vulnerability to stress and response to antidepressants. *Neuron 65*, 40−52.

(4) Popa, D., Cerdan, J., Reperant, C., Guiard, B. P., Guilloux, J. P., David, D. J., and Gardier, A. M. (2010) A longitudinal study of 5-HT outflow during chronic fluoxetine treatment using a new technique of chronic microdialysis in a highly emotional mouse strain. *Eur. J. Pharmacol. 628*, 83−90.

(5) Mathews, T. A., Fedele, D. E., Coppelli, F. M., Avila, A. M., Murphy, D. L., and Andrews, A. M. (2004) Gene dose-dependent alterations in extraneuronal serotonin but not dopamine in mice with reduced serotonin transporter expression. *J. Neurosci. Methods 140*, 169−181.

(6) Luellen, B. A., Bianco, L. E., Schneider, L. M., and Andrews, A. M. (2007) Reduced brain-derived neurotrophic factor is associated with a loss of serotonergic innervation in the hippocampus of aging mice. *Genes, Brain Behav. 6*, 482−490.

(7) Guiard, B. P., David, D. J., Deltheil, T., Chenu, F., Le Maitre, E., Renoir, T., Leroux-Nicollet, I., Sokoloff, P., Lanfumey, L., Hamon, M., Andrews, A. M., Hen, R., and Gardier, A. M. (2008) Brain-derived neurotrophic factor-deficient mice exhibit a hippocampal hyperserotonergic phenotype. *Int. J. Neuropsychopharmacol. 11*, 79−92.

(8) Staiti, A. M., Morgane, P. J., Galler, J. R., Grivetti, J. Y., Bass, D. C., and Mokler, D. J. (2011) A microdialysis study of the medial prefrontal cortex of adolescent and adult rats. *Neuropharmacology 61*, 544−549.

(9) Linthorst, A. C., and Reul, J. M. (2008) Stress and the brain: Solving the puzzle using microdialysis. *Pharmacol., Biochem. Behav. 90*, 163−173.

(10) Cadogan, A. K., Kendall, D. A., Fink, H., and Marsden, C. A. (1994) Social interaction increases 5-HT release and cAMP efflux in the rat ventral hippocampus in vivo. *Behav. Pharmacol. 5*, 299−305.

(11) Lada, M. W., Vickroy, T. W., and Kennedy, R. T. (1998) Evidence for neuronal origin and metabotropic receptor-mediated regulation of extracellular glutamate and aspartate in rat striatum in vivo following electrical stimulation of the prefrontal cortex. *J. Neurochem. 70*, 617−625.

(12) Song, P., Hershey, N. D., Mabrouk, O. S., Slaney, T. R., and Kennedy, R. T. (2012) Mass spectrometry "sensor" for in vivo acetylcholine monitoring. *Anal. Chem. 84*, 4659−4664.

(13) Vander Weele, C. M., Porter-Stransky, K. A., Mabrouk, O. S., Lovic, V., Singer, B. F., Kennedy, R. T., and Aragona, B. J. (2014) Rapid dopamine transmission within the nucleus accumbens: Dramatic difference between morphine and oxycodone delivery. *Eur. J. Neurosci. 40*, 3041−3054.

(14) Lorrain, D. S., Matuszewich, L., Friedman, R. D., and Hull, E. M. (1997) Extracellular serotonin in the lateral hypothalamic area is increased during the postejaculatory interval and impairs copulation in male rats. *J. Neurosci. 17*, 9361−9366.

(15) Richter, D. W., Schmidt-Garcon, P., Pierrefiche, O., Bischoff, A. M., and Lalley, P. M. (1999) Neurotransmitters and neuromodulators controlling the hypoxic respiratory response in anaesthetized cats. *J. Physiol. 514* (Pt 2), 567−578.

(16) Yoshitake, T., Fujino, K., Kehr, J., Ishida, J., Nohta, H., and Yamaguchi, M. (2003) Simultaneous determination of norepinephrine, serotonin, and 5-hydroxyindole-3-acetic acid in microdialysis samples from rat brain by microbore column liquid chromatography with fluorescence detection following derivatization with benzylamine. *Anal. Biochem. 312*, 125−133.

(17) Beekman, M., Flachskamm, C., and Linthorst, A. C. (2005) Effects of exposure to a predator on behaviour and serotonergic neurotransmission in different brain regions of C57bl/6N mice. *Eur. J. Neurosci. 21*, 2825−2836.

(18) Ma, F. R., Liu, J. X., Li, X. P., Mao, J. J., Zhang, Q. D., Jia, H. B., Mao, L. Q., and Zhao, R. (2007) Effects of caloric vestibular stimulation on serotoninergic system in the media vestibular nuclei of guinea pigs. *Chin. Med. J. (Engl.) 120*, 120−124.

(19) Yang, H., Thompson, A. B., McIntosh, B. J., Altieri, S. C., and Andrews, A. M. (2013) Physiologically relevant changes in serotonin resolved by fast microdialysis. *ACS Chem. Neurosci. 4*, 790−798.

(20) Liu, Y., Zhang, J., Xu, X., Zhao, M. K., Andrews, A. M., and Weber, S. G. (2010) Capillary ultrahigh performance liquid chromatography with elevated temperature for sub-one minute separations of basal serotonin in submicroliter brain microdialysate samples. *Anal. Chem. 82*, 9611−9616.

(21) Zhang, J., Liu, Y., Jaquins-Gerstl, A., Shu, Z., Michael, A. C., and Weber, S. G. (2012) Optimization for speed and sensitivity in capillary high performance liquid chromatography. The importance of column diameter in online monitoring of serotonin by microdialysis. *J. Chromatogr. A 1251*, 54−62.

(22) Zhang, J., Jaquins-Gerstl, A., Nesbitt, K. M., Rutan, S. C., Michael, A. C., and Weber, S. G. (2013) In vivo monitoring of serotonin in the striatum of freely moving rats with one minute temporal resolution by online microdialysis-capillary high-performance liquid chromatography at elevated temperature and pressure. *Anal. Chem. 85*, 9889−9897.

(23) Mokler, D. J., Lariviere, D., Johnson, D. W., Theriault, N. L., Bronzino, J. D., Dixon, M., and Morgane, P. J. (1998) Serotonin neuronal release from dorsal hippocampus following electrical stimulation of the dorsal and median raphe nuclei in conscious rats. *Hippocampus 8*, 262−273.

(24) Tossman, U., and Ungerstedt, U. (1986) The effect of apomorphine and pergolide on the potassium-evoked overflow of GABA in rat striatum studied by microdialysis. *Eur. J. Pharmacol. 123*, 295−298.

(25) Tossman, U., Jonsson, G., and Ungerstedt, U. (1986) Regional distribution and extracellular levels of amino acids in rat central nervous system. *Acta Physiol. Scand. 127*, 533−545.

(26) Shim, I., Javaid, J. I., and Kim, S. E. (2000) Effect of ginseng total saponin on extracellular dopamine release elicited by local infusion of nicotine into the striatum of freely moving rats. *Planta Med. 66*, 705−708.

(27) Fuentealba, J. A., Gysling, K., Magendzo, K., and Andres, M. E. (2006) Repeated administration of the selective kappa-opioid receptor agonist U-69593 increases stimulated dopamine extracellular levels in the rat nucleus accumbens. *J. Neurosci. Res. 84*, 450−459.

(28) Shi, X. R., Chang, J., Ding, J. H., Fan, Y., Sun, X. L., and Hu, G. (2008) Kir6.2 knockout alters neurotransmitter release in mouse striatum: An in vivo microdialysis study. *Neurosci. Lett. 439*, 230−234.

DOI: 10.1021/acschemneuro.5b00132
ACS Chem. Neurosci. 2015, 6, 1487−1501

(29) Bosse, K. E., Maina, F. K., Birbeck, J. A., France, M. M., Roberts, J. J., Colombo, M. L., and Mathews, T. A. (2012) Aberrant striatal dopamine transmitter dynamics in brain-derived neurotrophic factor-deficient mice. *J. Neurochem. 120*, 385−395.
(30) Clayton, J. A., and Collins, F. S. (2014) Policy: NIH to balance sex in cell and animal studies. *Nature 509*, 282−283.
(31) Bengel, D., Murphy, D. L., Andrews, A. M., Wichems, C. H., Feltner, D., Heils, A., Mossner, R., Westphal, H., and Lesch, K. P. (1998) insensitivity to 3,4-methylenedioxymethamphetamine ("Ecstasy") in serotonin transporter-deficient mice. *Mol. Pharmacol. 53*, 649−655.
(32) Gundlah, C., Simon, L. D., and Auerbach, S. B. (1998) Differences in hypothalamic serotonin between estrous phases and gender: An in vivo microdialysis study. *Brain Res. 785*, 91−96.
(33) Yorgason, J. T., Espana, R. A., and Jones, S. R. (2011) Demon voltammetry and analysis software: Analysis of cocaine-induced alterations in dopamine signaling using multiple kinetic measures. *J. Neurosci. Methods 202*, 158−164.
(34) Ferris, M. J., Calipari, E. S., Mateo, Y., Melchior, J. R., Roberts, D. C., and Jones, S. R. (2012) Cocaine self-administration produces pharmacodynamic tolerance: Differential effects on the potency of dopamine transporter blockers, releasers, and methylphenidate. *Neuropsychopharmacology 37*, 1708−1716.
(35) Calipari, E. S., Ferris, M. J., Salahpour, A., Caron, M. G., and Jones, S. R. (2013) Methylphenidate amplifies the potency and reinforcing effects of amphetamines by increasing dopamine transporter expression. *Nat. Commun. 4*, 2720.
(36) Dankoski, E. C., and Wightman, R. M. (2013) Monitoring serotonin signaling on a subsecond time scale. *Front. Integr. Neurosci. 7*, 44.
(37) Ferris, M. J., Calipari, E. S., Yorgason, J. T., and Jones, S. R. (2013) Examining the complex regulation and drug-induced plasticity of dopamine release and uptake using voltammetry in brain slices. *ACS Chem. Neurosci. 4*, 693−703.
(38) Street, S. E., Kramer, N. J., Walsh, P. L., Taylor-Blake, B., Yadav, M. C., King, I. F., Vihko, P., Wightman, R. M., Millan, J. L., and Zylka, M. J. (2013) Tissue-nonspecific alkaline phosphatase acts redundantly with PAP and NT5E to generate adenosine in the dorsal spinal cord. *J. Neurosci. 33*, 11314−11322.
(39) Calipari, E. S., Ferris, M. J., Melchior, J. R., Bermejo, K., Salahpour, A., Roberts, D. C., and Jones, S. R. (2014) Methylphenidate and cocaine self-administration produce distinct dopamine terminal alterations. *Addict. Biol. 19*, 145−155.
(40) Sanchez, C., Bergqvist, P. B., Brennum, L. T., Gupta, S., Hogg, S., Larsen, A., and Wiborg, O. (2003) Escitalopram, the S-(+)-enantiomer of citalopram, is a selective serotonin reuptake inhibitor with potent effects in animal models predictive of antidepressant and anxiolytic activities. *Psychopharmacology (Berl.) 167*, 353−362.
(41) Stahl, S. M. (2004) Selectivity of SSRIs: Individualising patient care through rational treatment choices. *Int. J. Psychiatry Clin. Pract. 8* (Suppl. 1), 3−10.
(42) Zhou, M., Engel, K., and Wang, J. (2007) Evidence for significant contribution of a newly identified monoamine transporter (PMAT) to serotonin uptake in the human brain. *Biochem. Pharmacol. 73*, 147−154.
(43) Baganz, N. L., Horton, R. E., Calderon, A. S., Owens, W. A., Munn, J. L., Watts, L. T., Koldzic-Zivanovic, N., Jeske, N. A., Koek, W., Toney, G. M., and Daws, L. C. (2008) Organic cation transporter 3: Keeping the brake on extracellular serotonin in serotonin-transporter-deficient mice. *Proc. Natl. Acad. Sci. U. S. A. 105*, 18976−18981.
(44) Daws, L. C. (2009) Unfaithful neurotransmitter transporters: Focus on serotonin uptake and implications for antidepressant efficacy. *Pharmacol. Ther. 121*, 89−99.
(45) Wood, K. M., and Hashemi, P. (2013) Fast-scan cyclic voltammetry analysis of dynamic serotonin reponses to acute escitalopram. *ACS Chem. Neurosci. 4*, 715−720.
(46) Zhou, F. C., Lesch, K. P., and Murphy, D. L. (2002) Serotonin uptake into dopamine neurons via dopamine transporters: A compensatory alternative. *Brain Res. 942*, 109−119.
(47) Altieri, S. C., Yang, H., O'Brien, H. J., Redwine, H. M., Senturk, D., Hensler, J. G., and Andrews, A. M. (2015) Perinatal vs. genetic programming of adult serotonin states associated with anxiety. *Neuropsychopharmacology 40*, 1456−1470.
(48) Kim, D. K., Tolliver, T. J., Huang, S. J., Martin, B. J., Andrews, A. M., Wichems, C., Holmes, A., Lesch, K. P., and Murphy, D. L. (2005) Altered serotonin synthesis, turnover and dynamic regulation in multiple brain regions of mice lacking the serotonin transporter. *Neuropharmacology 49*, 798−810.
(49) Borue, X., Condron, B., and Venton, B. J. (2010) Both synthesis and reuptake are critical for replenishing the releasable serotonin pool in Drosophila. *J. Neurochem. 113*, 188−199.
(50) Li, Q., Wichems, C., Heils, A., Lesch, K. P., and Murphy, D. L. (2000) Reduction in the density and expression, but not G-protein coupling of serotonin receptors (5-HT1A) in 5-HT transporter knockout mice: Gender and brain region differences. *J. Neurosci. 20*, 7888−7895.
(51) Jennings, K. A., Lesch, K. P., Sharp, T., and Cragg, S. J. (2010) Non-linear relationship between 5-HT transporter gene expression and frequency sensitivity of 5-HT signals. *J. Neurochem. 115*, 965−973.
(52) Maswood, S., Truitt, W., Hotema, M., Caldarola-Pastuszka, M., and Uphouse, L. (1999) Estrous cycle modulation of extracellular serotonin in mediobasal hypothalamus: Role of the serotonin transporter and terminal autoreceptors. *Brain Res. 831*, 146−154.
(53) Lu, N. Z., Eshleman, A. J., Janowsky, A., and Bethea, C. L. (2003) Ovarian steroid regulation of serotonin reuptake transporter (SERT) binding, distribution, and function in female macaques. *Mol. Psychiatry 8*, 353−360.
(54) Sanchez, M. G., Morissette, M., and Di Paolo, T. (2013) Oestradiol modulation of serotonin reuptake transporter and serotonin metabolism in the brain of monkeys. *J. Neuroendocrinol. 25*, 560−569.
(55) Sanchez, M. G., Morissette, M., and Di Paolo, T. (2013) Estradiol and brain serotonin reuptake transporter in long-term ovariectomized parkinsonian monkeys. *Prog. Neuro-Psychopharmacol. Biol. Psychiatry 45*, 170−177.
(56) Bevins, R. A., and Charntikov, S. (2015) We know very little about the subjective effects of drugs in females. *ACS Chem. Neurosci. 6*, 359−361.
(57) Bungay, P. M., Morrison, P. F., Dedrick, R. L., Chefer, V. I., and Zapata, A. (2007) *Principles of Quantitative Microdialysis* (Westerink, B. H., and Cremers, T. I., Eds.), pp 131−168, Elsevier B. V., The Netherlands.
(58) Olson Cosford, R. J., Vinson, A. P., Kukoyi, S., and Justice, J. B., Jr. (1996) Quantitative microdialysis of serotonin and norepinephrine: Pharmacological influences on *in vivo* extraction fraction. *J. Neurosci. Methods 68*, 39−47.
(59) Yang, H., Peters, J. L., Allen, C., Chern, S. S., Coalson, R. D., and Michael, A. C. (2000) A theoretical description of microdialysis with mass transport coupled to chemical events. *Anal. Chem. 72*, 2042−2049.
(60) Bungay, P. M., Dedrick, R. L., Fox, E., and Balis, F. M. (2001) Probe calibration in transient microdialysis in vivo. *Pharm. Res. 18*, 361−366.
(61) Kennedy, R. T. (2013) Emerging trends in in vivo neurochemical monitoring by microdialysis. *Curr. Opin. Chem. Biol. 17*, 860−867.
(62) Sarter, M., and Kim, Y. (2015) Interpreting chemical neurotransmission in vivo: Techniques, time scales, and theories. *ACS Chem. Neurosci. 6*, 8−10.
(63) Murphy, D. L., Fox, M. A., Timpano, K. R., Moya, P. R., Ren-Patterson, R., Andrews, A. M., Holmes, A., Lesch, K. P., and Wendland, J. R. (2008) How the serotonin story is being rewritten by new gene-based discoveries principally related to *SLC6A4*, the serotonin transporter gene, which functions to influence all cellular serotonin systems. *Neuropharmacology 55*, 932−960.

DOI: 10.1021/acschemneuro.5b00132
ACS Chem. Neurosci. 2015, 6, 1487−1501

(64) Murphy, D. L., and Lesch, K. P. (2008) Targeting the murine serotonin transporter: Insights into human neurobiology. *Nat. Rev. Neurosci. 9*, 85−96.
(65) Bungay, P. M., Morrison, P. F., and Dedrick, R. L. (1990) Steady-state theory for quantitative microdialysis of solutes and water in vivo and in vitro. *Life Sci. 46*, 105−119.
(66) Peters, J. L., and Michael, A. C. (1998) Modeling voltammetry and microdialysis of striatal extracellular dopamine: The impact of dopamine uptake on extraction and recovery ratios. *J. Neurochem. 70*, 594−603.
(67) Bungay, P. M., Newton-Vinson, P., Isele, W., Garris, P. A., and Justice, J. B. (2003) Microdialysis of dopamine interpreted with quantitative model incorporating probe implantation trauma. *J. Neurochem. 86*, 932−946.
(68) Chen, K. C. (2005) Evidence on extracellular dopamine level in rat striatum: Implications for the validity of quantitative microdialysis. *J. Neurochem. 92*, 46−58.
(69) Anisman, H., and Zacharko, R. M. (1986) Behavioral and neurochemical consequences associated with stressors. *Ann. N. Y. Acad. Sci. 467*, 205−225.
(70) Fink, G., Sumner, B. E., Rosie, R., Grace, O., and Quinn, J. P. (1996) Estrogen control of central neurotransmission: Effect on mood, mental state, and memory. *Cell. Mol. Neurobiol. 16*, 325−344.
(71) Berretta, N., Nistico, R., Bernardi, G., and Mercuri, N. B. (2008) Synaptic plasticity in the basal ganglia: A similar code for physiological and pathological conditions. *Prog. Neurobiol. 84*, 343−362.
(72) Lobo, M. K., and Nestler, E. J. (2011) The striatal balancing act in drug addiction: Distinct roles of direct and indirect pathway medium spiny neurons. *Front. Neuroanat. 5*, 41.
(73) Hart, G., Leung, B. K., and Balleine, B. W. (2014) Dorsal and ventral streams: The distinct role of striatal subregions in the acquisition and performance of goal-directed actions. *Neurobiol. Learn. Mem. 108*, 104−118.
(74) McLean, A. C., Valenzuela, N., Fai, S., and Bennett, S. A. (2012) Performing vaginal lavage, crystal violet staining, and vaginal cytological evaluation for mouse estrous cycle staging identification. *J. Visualized Exp.*, e4389.

DOI: 10.1021/acschemneuro.5b00132
ACS Chem. Neurosci. 2015, 6, 1487−1501